Title

Morphogen Delivery by Osteoconductive Nanoparticles Instructs Stromal Cell Spheroid Phenotype

Journal

Advanced Biology, 3(12)

ISSN

2701-0198

Authors

Whitehead, Jacklyn
Kothambawala, Alefia
Leach, J Kent

Publication Date

2019-12-01

DOI

10.1002/adbi.201900141

Peer reviewed

Published in final edited form as:

Adv Biosyst. 2019 December ; 3(12): . doi:10.1002/adbi.201900141.

Morphogen Delivery by Osteoconductive Nanoparticles Instructs Stromal Cell Spheroid Phenotype

Jacklyn Whitehead, **Alefia Kothambawala**

Department of Biomedical Engineering, University of California, Davis, CA 95616

J. Kent Leach

Department of Biomedical Engineering, University of California, Davis, CA 95616

Department of Orthopaedic Surgery, UC Davis Health, Sacramento, CA 95817

Abstract

Mesenchymal stem/stromal cells (MSCs) exhibit a rapid loss in osteogenic phenotype upon removal of osteoinductive cues, as commonly occurs during transplantation. Osteogenic differentiation can be more effectively but not fully maintained by aggregating MSCs into spheroids. Therefore, the development of effective strategies that prolong the efficacy of inductive growth factors would be advantageous for advancing cell-based therapies. To address this challenge, osteoinductive bone morphogenetic protein-2 (BMP-2) was adsorbed to osteoconductive hydroxyapatite (HA) nanoparticles for incorporation into MSC spheroids. MSC induction was evaluated in osteogenic conditions and retention of the osteogenic phenotype in the absence of other osteogenic cues. HA was more uniformly incorporated into spheroids at lower concentrations, while BMP-2 dosage was dependent upon initial morphogen concentration. MSC spheroids containing BMP-2-loaded HA nanoparticles exhibited greater alkaline phosphatase (ALP) activity and more uniform spatial expression of osteocalcin compared to spheroids with uncoated HA nanoparticles. Spheroids cultured in media containing soluble BMP-2 demonstrated differentiation only at the spheroid periphery. Furthermore, the osteogenic phenotype of MSC spheroids was better retained with BMP-2-laden HA upon the removal of soluble osteogenic cues. These findings represent a promising strategy for simultaneous delivery of osteoconductive and osteoinductive signals for enhancing MSC participation in bone formation.

Graphical Abstract

jkleach@ucdavis.edu.

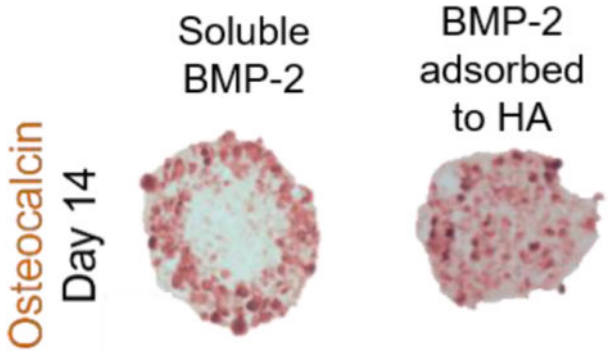

Mesenchymal stem/stromal cells (MSCs) exhibit a rapid loss in osteogenic phenotype upon removal of osteoinductive cues. Osteogenic differentiation can be more effectively maintained by aggregating MSCs into spheroids and incorporating adsorbed osteoinductive bone morphogenetic protein-2 (BMP-2) to osteoconductive hydroxyapatite (HA) nanoparticles. This method yields more uniform expression of osteogenic markers compared to spheroids induced with soluble BMP-2 in culture media.

Keywords

Spheroids; osteogenesis; BMP-2; hydroxyapatite; mesenchymal stem/stromal cells

1. Introduction

Mesenchymal stem/stromal cells (MSCs) are a promising source for cell-based therapies due to their availability from numerous tissue compartments, trophic factor secretion, and potential to differentiate toward several phenotypes in the presence of specific bioactive cues.[1] However, MSC-based therapies for bone regeneration have limited efficacy due to high rates of cell death upon transplantation.[2] The therapeutic effectiveness of MSCs can be increased through aggregation into spheroids, which does not hinder the multipotency of MSCs.[3] Compared to monolayer culture or monodispersed cells, spheroids exhibit enhanced cell survival, increased secretion of proangiogenic and anti-inflammatory factors, improved ability to sustain an acquired phenotype, and offer a more physiologically relevant microenvironment for cells.[4, 5]

MSCs are commonly induced toward an osteogenic phenotype using a cocktail of soluble osteogenic cues. However, we and others have shown that MSCs can dedifferentiate upon removal of osteoinductive supplements[6, 7], as commonly occurs upon transplantation. Regardless of induction duration, MSCs in monolayer culture exhibited a loss of osteogenic markers within 24 hours of stimulus withdrawal.[6] The retention of phenotype can be improved with aggregation into spheroids, yet reductions in the phenotype are still observed 5 days after stimulus removal.[5] These data suggest that the soluble cues from an osteogenic cocktail of factors are insufficient to lock MSCs into an osteogenic phenotype. Additionally, cues added to the culture media are only available to cells on the periphery of a spheroid, potentially enhancing the heterogeneous nature of aggregates and resulting in cells with varying degrees of differentiation within the spheroid. Thus, there is a significant need to

develop alternative means to induce and retain the osteogenic phenotype in MSCs throughout the spheroidal structure.

Bone morphogenetic protein-2 (BMP-2) is a potent osteoinductive cue that is broadly used to influence osteogenic differentiation or augment the traditional soluble cocktail of osteogenic supplements.[8] However, numerous contraindications have been associated with BMP-2, including ectopic bone formation, inflammation, and stimulation of cancer cells due to the supraphysiological dosages required to achieve bone formation in humans.[9] These challenges are primarily related to the ineffectiveness of many delivery vehicles. Osteoconductive carriers provide sites for protein and cell adhesion, as well as nucleation sites for cell-secreted calcium to enhance formation of mineralized tissue. Hydroxyapatite (HA) is an osteoconductive, biocompatible ceramic and the main mineral component of bone.[10] The biophysical properties of HA facilitate protein adsorption onto its surface.[11] Hence, an osteoconductive drug delivery vehicle that enables the presentation of small, targeted morphogen dosages would further increase the advantages of BMP-2 delivery for use in bone tissue engineering.

Herein, we demonstrate that the localized delivery of BMP-2 from HA nanoparticles within MSC spheroids can promote and retain the osteogenic phenotype. We adsorbed BMP-2 to HA and formed MSC spheroids in the presence of these nanoparticles to achieve improved spatial distribution of BMP-2 within the aggregate. We examined the osteogenic response of MSC spheroids, as well as the retention of the acquired osteogenic phenotype of MSC spheroids in the absence of sustained osteoinductive cues. These data demonstrate that HA nanoparticles are effective delivery vehicles for osteoinductive cues that promote and sustain the osteogenic phenotype throughout the spheroid structure.

2. Results

2.1 MSC spheroid morphology and diameter are influenced by HA concentration

We incorporated HA into MSC spheroids during the aggregation process to present osteoinductive and osteoconductive cues throughout the spheroid (Figure 1A). We examined various concentrations of HA to identify the mass that could be successfully incorporated into spheroids and still retain the aggregate morphology. The gross morphology and diameter of the spheroids was influenced by HA concentration (Figure 1B). However, the DNA content, an indicator of cell number, remained unchanged despite HA loading (Figure 1C). MSCs could successfully aggregate in the presence of HA (Figure 1D) and maintain their spheroidal morphology at HA concentrations up to 1.0 mg/mL. As spheroid morphology was not retained with the incorporation of HA nanoparticles at 1.5 mg/mL, exhibited by less compact spherical morphology, this concentration was excluded from the remainder of our studies.

2.2 HA distribution within MSC spheroids is dependent on loading concentration

We examined the spatial distribution of HA within MSC spheroids after spheroid formation. Under H&E staining, we observed voids within spheroids (Figure 2A), and the size and frequency of those voids increased with HA concentration. We confirmed that these voids

were caused by HA with Alizarin Red staining (Supplementary Figure 1). Upon examination with scanning electron microscopy, the gross morphology of the HA nanoparticles exhibited aggregation (Figure 2B). These findings are in agreement with our quantification of HA nanoparticle diameter using dynamic light scattering (Figure 2C). HA aggregation was more pronounced at higher concentrations.

2.3 BMP-2 is observable within MSC spheroids when adsorbed onto HA

We evaluated BMP-2 distribution within spheroids by incorporating fluorescently labeled BMP-2 adsorbed to HA during formation (Figure 3A). Spheroids containing only HA exhibited low fluorescence intensity. Spheroids formed with HA and incubated with soluble BMP-2 in the culture media had slightly higher, yet still low fluorescent intensity. Spheroids formed with BMP-2-laden HA exhibited pronounced fluorescence intensity localized within the MSC spheroids (Figure 3B). These observations were confirmed by quantification of the relative fluorescence intensity (Figure 3C). Interestingly, we did not observe any significant differences in relative fluorescence intensity of the labeled BMP-2 among the different concentrations of HA.

2.4 Measurement of BMP-2 loading and bioactivity on HA nanoparticles

We measured the quantity of BMP-2 adsorbed onto HA to determine the dosage presented to MSC spheroids (Figure 4A). Regardless of HA concentration, 100 ng/mL of BMP-2 incubated in the presence of HA resulted in the adsorption of 36.4 ± 13.1 ng/mL of BMP-2. Using an initial concentration of 200 ng/mL BMP-2, we detected a range of adsorption efficiencies with variable HA concentrations. Specifically, 46.6 ± 7.6 ng/mL of BMP-2 was absorbed onto 0.1 mg/mL of HA, 91.2 ± 17.5 ng/mL was absorbed onto 0.5 mg/mL of HA, and 154.0 ± 18.1 ng/mL was absorbed onto 1.0 mg/mL of HA. When starting with 300 ng/mL BMP-2, 104.2 ± 19.5 ng/mL of BMP-2 was adsorbed across all concentrations of HA. We selected 200 ng/mL of BMP-2 for the remainder of our studies because there was a high rate of adsorption that varied with HA concentration.

We evaluated the bioactivity of adsorbed BMP-2 using spheroids formed of W-20–17 cells, the industry standard for testing recombinant BMP-2. Groups are described in Table 1, and all groups using W-20–17 cells contained osteogenic media. ALP activity was increased in all groups containing BMP-2 HA compared to groups with BMP-2 in the culture media (Figure 4B). Spheroids containing 0.1 mg/mL of BMP-2-laden HA nanoparticles exhibited the greatest ALP activity, with 0.5 mg/mL exhibiting a statistically similar response.

2.5 Spheroid DNA content, metabolic activity, and viability are unaffected by BMP-2 and HA treatment

HA concentration had no appreciable effect on the viability of MSC spheroids over 14 days. Spheroid DNA content (Supplementary Figure 2A), metabolic activity (Supplementary Figure 2B), and viability (Supplementary Figure 2C) were similar among all treatment groups.

2.6 Localized BMP-2 delivery from HA nanoparticles promotes osteogenic differentiation throughout the spheroid

We then tested the osteogenic induction of MSC spheroids when formed with BMP-2-loaded HA (Figure 5A) by evaluating *IBSP* expression, ALP activity, collagen content, and osteocalcin expression. After 7 days in osteogenic culture, we observed the highest expression of *IBSP* in BMP-2 HA at 0.1 mg/mL (Figure 5B). MSC spheroids containing BMP-2 adsorbed onto 0.5 mg/mL of HA had approximately one-half the expression achieved with 0.1 mg/mL ($p<0.0001$). Similarly, spheroids with 0.1 mg/mL of BMP-2 HA had the greatest ALP activity (Figure 5C) after 7 days (18.5 ± 1.4 units/ng), which was comparable to spheroids with 0.5 mg/mL of BMP-2 HA (15.1 ± 3.0 units/ng; p=0.51). MSC spheroids containing 0.1 mg/mL BMP-2 HA had significantly higher ALP activity than groups lacking BMP-2 adsorbed onto HA. Picrosirius red staining, an indicator of collagen content, was most prevalent in MSC spheroids containing 0.1 mg/mL BMP-2 HA and HA-containing spheroids with soluble BMP-2 (OMHA Sol BMP) (Figure 5D). We detected the most intense, spatially homogeneous osteocalcin staining in spheroids containing 0.1 and 0.5 mg/mL BMP-2 HA. In contrast, OMHA Sol BMP spheroids exhibited osteocalcin staining restricted to the periphery.

2.7 Localized BMP-2 delivery by HA enhances the retention of the osteogenic phenotype after removal of soluble osteogenic cues

We tested the retention of the osteogenic phenotype in MSCs (Figure 6A) by comparing the ability of spheroids to maintain the induced osteogenic phenotype when cultured for 5 days in growth medium lacking additional osteogenic supplements. Calcium deposition was highest in all groups containing HA compared to MSCs primed in osteogenic media (OM) alone. These induced cells had almost no measurable calcium after 5 days in culture without soluble osteoinductive cues (Figure 6B). When expressed as a percentage of the initial Day 0 calcium value, MSC spheroids formed with 0.1 mg/mL HA had the most retained calcium at 48.2 ± 10.5% (Figure 6C), while OMHA Sol BMP MSC spheroids retained 36.9 ± 6.0% of initial calcium mass. We compared *RUNX2* expression of OM-treated spheroids to all other groups 5 days after osteogenic supplements were removed. We detecteds greater expression of this early osteogenic marker in all groups with BMP-2 adsorbed to HA nanoparticles (Figure 6D). *RUNX2* expression was highest in spheroids containing 0.5 mg/mL of BMP-2 loaded HA. In agreement with MSCs undergoing osteogenic induction, spheroids treated with soluble BMP-2 and then maintained in growth media for 5 days exhibited more profound collagen (top) and osteocalcin (bottom) (Figure 6E) expression at the periphery. In contrast, MSC spheroids formed with 0.1 mg/mL BMP-2 HA possessed more homogeneous expression of both picrosirius red and osteocalcin throughout the spheroid.

3. Discussion

Osteogenic differentiation of MSC spheroids requires uniform induction that is retained throughout the cell aggregate to be effective for *in vivo* transplantation and subsequent bone formation. This study explored the capacity of MSC spheroids loaded with BMP-2-adsorbed HA nanoparticles to augment induction of osteogenesis and prolong retention of the acquired osteogenic phenotype. MSC spheroids containing HA have promising implications

for bone tissue engineering applications, as they address targeted delivery to intended cells, facilitate delivery of a potent growth factor on a nanoscale particle with osteoconductive properties, and offer an alternative method to deliver growth factors versus freely soluble cues eluting from a carrier. Furthermore, this process does not interfere with cell-cell and cell-extracellular matrix connections within spheroids, increasing cell survival, and mimicking a more physiologically relevant microenvironment.

BMP-2 is one of the most potent osteoinductive cues for MSC differentiation.[12] The translational feasibility of BMP-2 in a regenerative therapy to enable new bone formation necessitates long-term presentation of the growth factor to cells directly at the site of injury. A host of methods have been investigated to use small BMP-2 doses and control its delivery before it undergoes proteolytic degradation.[13] Local presentation of BMP-2 from engineered carriers suffers from challenges in achieving the desired release kinetics, duration of presentation, or insufficient targeting to responsive cells. Herein, the adsorption of BMP-2 onto HA nanoparticles for immediate incorporation into MSC spheroids ensures that BMP-2 will be presented directly to the cells of interest at a small, targeted dosage.

Ceramic delivery systems, particularly HA, have been effectively utilized to deliver various biomolecules including amino acids, hormones, proteins, genes, and antibiotics.[14] We focused on using HA as both a delivery vehicle and an osteoconductive material to enhance osteogenic differentiation. Others have used mineral-coated HA microparticles to deliver BMP-2 directly to larger (approximately 1 mm) MSC aggregates via plasmid delivery[15] or in combination with other factors following a prolonged adhesion period.[16] This strategy was pursued to stimulate endochondral ossification, which is the primary mechanism of bone formation in the appendicular skeleton. In an effort to promote the direct osteogenic differentiation of MSCs, as occurs in the craniomaxillofacial region, we examined the ability of BMP-2-adsorbed HA to induce MSC osteogenic differentiation and retain the osteogenic phenotype.

The use of a delivery vehicle on the nanoparticle scale allows for MSCs within the spheroid to maintain their cell-cell contacts. The significance of cadherins on MSC spheroid formation and enhanced survival has been previously reported,[17] and our lab has demonstrated the importance of the cell-extracellular matrix interaction on the commitment to the osteogenic phenotype.[5] Therefore, it is critical to maintain spheroidal architecture in order to reap the benefits of aggregated culture that promotes cell-cell interactions. Others have successfully incorporated larger ceramic microparticles to promote the desired phenotype.[18] However, the spatial uniformity throughout a three-dimensional cell aggregate is more easily achievable with nanoscale, rather than macroscale, particles.

The prevailing paradigm for MSC efficacy in cell-based therapies is indirect contribution by secretion of bioactive factors instead of directly contributing to bone formation through osteoblastic differentiation.[19] We and others have shown that aggregation of MSCs into spheroids provides exciting opportunities to increase MSC participation in bone formation.[1] This study demonstrates the utility of a delivery system that further enhances the efficacy of MSC spheroids for direct use in regenerative therapies by both inducing and retaining the phenotype using an osteoinductive (BMP-2) and an osteoconductive (HA) factor. BMP-2

and HA appear to cooperatively enhance the bone-forming potential of MSCs. Others have also demonstrated that BMP-2 may provide an additive effect at low dosages.[21] We demonstrate a similar additive effect of BMP-2 and HA for more spatially uniform instruction throughout the spheroid and thus, advance the efficacy of direct MSC contribution to cell-based therapies.

In this study, we investigated the incorporation of BMP-2-loaded HA nanoparticles into MSC spheroids. We used a range of HA concentrations from 0.1 to 1.5 mg/mL. We did not pursue dosages of HA smaller than 0.1 mg/mL. Additionally, we only investigated 200 ng/mL of BMP-2 adsorbed onto HA and then subsequently incorporated into MSC spheroids. However, others have examined varying concentrations of BMP-2 delivered on a ceramic particle and determined that BMP-2 induces osteogenesis in a concentration-dependent manner.[18] We observed a plateau in BMP-2 adsorption to the HA nanoparticles, possibly due to saturation of the electrostatic attraction between BMP-2 and HA.[22] Furthermore, our HA nanoparticles exhibited clustering during the BMP-2 adsorption process. HA nanoparticles clustered at higher concentrations, and although more BMP-2 was adsorbed on higher concentrations of HA, we did not observe a corresponding increase in osteogenic markers. The access of MSCs to BMP-2 was potentially obscured due to HA clustering at higher concentrations, thereby limiting the osteoinductive effect. We could potentially achieve enhanced osteogenic induction and retention of the phenotype using ceramic particles that do not aggregate. Others have added magnesium to HA to control the orientation of the growth factor on the ceramic surface in an effort to augment HA as a morphogen delivery vehicle.[23] Thus, additional work is warranted to increase ceramic spatial distribution within the spheroid in the pursuit of a more uniform presentation of adsorbed BMP-2.

4. Conclusion

BMP-2-laden HA incorporation into the spheroids resulted in more uniform spatial expression of the osteogenic phenotype compared to the addition of BMP-2 in the culture medium. Lower concentrations of HA with adsorbed BMP-2 exhibited the greatest increase in gene expression and ALP activity for induction and the highest percentage of retained calcium in retention studies. All BMP-2-HA containing spheroids demonstrated an enhanced ability to sustain the osteogenic phenotype throughout the entire spheroid that was not limited to the periphery, as was the addition of soluble BMP-2. These data demonstrate the promise of using BMP-2-adsorbed HA nanoparticles incorporated into MSCs spheroids at low HA concentrations to enhance osteogenesis, minimize interference of cell-cell contacts, and further cell-based tissue engineering strategies for bone defect repair.

5. Experimental Section

Cell culture

Human bone marrow-derived MSCs (Texas A&M Institute for Regenerative Medicine, Temple, TX) were received at passage 2 and used without additional characterization. MSCs were expanded in standard culture conditions (37°C, 21% O_2, 5% CO_2) in α-MEM (Life Technologies, Carlsbad, CA) supplemented with 10% fetal bovine serum (FBS, Atlanta

Biologicals, Flowery Branch, GA) and 1% penicillin/streptomycin (P/S, Gemini Bio Products, Sacramento, CA) until use at passage 4–5. Murine W-20–17 cells (ATCC, Manassas, VA) were expanded in standard culture conditions in DMEM (Life Technologies) supplemented with 10% FBS and 1% P/S.

Spheroid formation

Spheroids were formed using a forced aggregation method.[24] Briefly, MSCs (4.35×10^5 cells/mL) were pipetted into agarose molds in well plates, and the well plates were centrifuged at 500×g for 8 min. Plates were maintained statically in standard culture conditions for 48 h to form spheroids. Each microwell contained 15,000 MSCs.

Human recombinant BMP-2 (Medtronic, Minneapolis, MN) was adsorbed onto HA nanoparticles (100 nm average diameter, Berkeley Advanced Biomaterials, Berkeley, CA) by resuspending HA in phosphate buffered saline (PBS, Thermo Fisher Scientific, Waltham, MA) and adding BMP-2 to a final concentration of 200 ng/mL in low adhesion conical tubes. After 90 min, the tubes were centrifuged at 500×g for 8 min, and the supernatant was aspirated, leaving the pelleted HA. The pellet was washed once with PBS, the mixture centrifuged again at 500×g for 8 min, and PBS was aspirated. The remaining pellet was resuspended in cell culture media for subsequent incorporation into spheroids.

HA was incorporated into spheroid cultures by resuspending the cell pellet of known cell number in media containing HA. The HA-cell mixture was pipetted up and down for 5 s to ensure homogeneity. The HA-cell suspension was then dispersed into the agarose molds and spheroids were formed as described above.

Spheroid characterization

The diameter of live spheroids was measured using brightfield microscopy (Nikon Eclipse TE2000U microscope, Melville, NY). Spheroid diameter was calculated using NIS Elements (Nikon) by averaging the major and minor axis. Cell viability was assessed by a Live/Dead assay (Life Technologies). To measure cellular metabolic activity, spheroids were transferred to 24 well plates and incubated in 500 μL of α-MEM containing 10% v/v alamarBlue (Thermo Fisher) for 30 min. MSC spheroids were washed and subsequently collected in passive lysis buffer (Promega, Madison, WI), and DNA content was determined using the Quant-iT PicoGreen DNA Assay Kit (Invitrogen, Carlsbad, CA).

HA nanoparticle characterization

The gross morphology of HA nanoparticles was visualized at 10 kV using scanning electron microscopy (SEM, Hitachi 3500-N, Hitachi Science Systems Ltd, Tokyo, Japan). Diameter of the particles was determined using dynamic light scattering on a Nano-ZS90 Zetasizer (Malvern, Westborough, MA). Nanoparticles were dissolved at either 0.1, 0.5, or 1.0 mg/mL in PBS in a disposable polystyrene cuvette and were subjected to a minimum of 16 runs. The average diameter from these runs was recorded and repeated three times for three replicates at each concentration.

Characterization and quantification of BMP-2 adsorption onto HA

We labeled BMP-2 using the Alexa Fluor 488 microscale protein labeling kit (Thermo Fisher) following the manufacturer's instructions. Fluorescently labeled BMP-2 was adsorbed onto HA and subsequently incorporated into spheroids as described above. Spheroids were imaged using both brightfield and fluorescent microscopy, and these images were overlaid to form a composite image. The relative fluorescence intensity of spheroids in the fluorescent channel was quantified using ImageJ.

In order to quantify morphogen loading, BMP-2 was eluted from the HA nanoparticles as previously reported.[25] We prepared an elution buffer composed of 2 mM $CaCl_2$ solution in N-2-hydroxyethyl-piperazine-N-2-ethanesulfonic acid (HEPES, Thermo Fisher) at pH 6.0. BMP-2-laden HA nanoparticles were incubated in the elution buffer for 40 min, and the supernatant was collected. BMP-2 concentration within the supernatant was quantified using human-specific enzyme-linked immunosorbent assay (ELISA) kits (R&D Systems, Minneapolis, MN).

Induction and retention of the osteogenic phenotype in MSC spheroids

For induction, MSCs were formed into spheroids and maintained in osteogenic media consisting of α-MEM supplemented with 50 μg/mL ascorbate-2-phosphate, 10 mM β-glycerophosphate, and 100 nM dexamethasone (all from Sigma-Aldrich, St. Louis, MO) for 14 days. For retention, MSCs underwent osteogenic differentiation using the aforementioned osteogenic medium for 12 days in monolayer culture. Spheroids were then formed in osteogenic media, for a total of 14 days of osteoinduction, after which media was refreshed with growth media. We measured intracellular alkaline phosphatase (ALP) activity as previously described.[26] Calcium deposition was quantified using a Stanbio™ Calcium Liquid Reagent kit (Thermo Fisher). All values are presented after subtracting initial calcium levels and accounting for HA as a calcium source. Gene expression was assessed by quantitative PCR. Total RNA was collected using the Trizol RNA isolation protocol (Thermo Fisher), and 600 ng of total RNA was reverse-transcribed with the QuantiTect Reverse Transcription Kit (Qiagen, Valencia, CA). qPCR was performed using TaqMan1 Universal PCR Master Mix (Thermo Fisher). Primers and probes consisted of *IBSP* (Hs00173720_m1), *RUNX2* (Hs00231692_m1), and *RPL13* (Hs00204173_m1) (Thermo Fisher). Quantitative PCR results were normalized to the housekeeping transcript level (*RPL13*) and the control value of OM to yield $2^{-\Delta\Delta Ct}$ [27] or the housekeeping transcript level to yield $2^{-\Delta Ct}$.

Spheroids were fixed in phosphate buffered formalin for 24 h at 4°C and then paraffin embedded. Sections were cut at 10 μm thickness and stained for hematoxylin and eosin (H&E), Alizarin Red for calcium, picrosirius red for collagen, or immunohistochemistry (IHC). For IHC, we used a primary antibody against osteocalcin (ab13420, 1:200, Abcam, Cambridge, MA) in conjugation with a mouse and rabbit-specific horseradish peroxidase (HRP)/3,3′-diaminobenzidine (DAB) detection kit (Abcam). Sections were imaged using a Nikon Eclipse TE2000U microscope.

Statistical analysis

All data represent a minimum of 3 independent experiments. Statistical analysis was performed using a one-way analysis of variance (ANOVA) with a Tukey's multiple comparison post hoc test, and all statistical analyses were performed using Prism 8 software (GraphPad, San Diego, CA). Data are presented as mean ± standard deviation with significant differences ($p<0.05$) indicated by groups not sharing the same letter. Groups with the same letter are not significantly different from one another, and groups with more than one letter reflect overlap between groups.

Supplementary Material

Refer to Web version on PubMed Central for supplementary material.

Acknowledgements

This work was supported by the National Institutes of Health under award number R01 DE025475 (JKL). JW was supported by a National Science Foundation Graduate Research Fellowship (1650042) and the Achievement Rewards for College Scientists (ARCS) Foundation fellowship. The content is solely the responsibility of the authors and does not necessarily represent the official views of the National Institutes of Health, National Science Foundation, or the ARCS Foundation.

References

[1]. Caplan AI, Correa D, Cell Stem Cell 2011, 9, 11. [PubMed: 21726829]

[2]. a)Moya A, Paquet J, Deschepper M, Larochette N, Oudina K, Denoeud C, Bensidhoum M, Logeart-Avramoglou D, Petite H, Stem Cells 2018, 36, 363; [PubMed: 29266629] b)Eggenhofer E, Luk F, Dahlke MH, Hoogduijn MJ, Front Immunol 2014, 5, 148. [PubMed: 24904568]

[3]. Alimperti S, Lei P, Wen Y, Tian J, Campbell AM, Andreadis ST, Biotechnol Progr 2014, 30, 974.

[4]. a)Bartosh TJ, Ylostalo JH, Mohammadipoor A, Bazhanov N, Coble K, Claypool K, Lee RH, Choi H, Prockop DJ, Proc Natl Acad Sci 2010, 107, 13724; [PubMed: 20643923] b)Ylöstalo JH, Bartosh TJ, Coble K, Prockop DJ, Stem Cells 2012, 30, 2283. [PubMed: 22865689]

[5]. Murphy KC, Hoch AI, Harvestine JN, Zhou D, Leach JK, Stem Cell Transl Med 2016, 5, 1229.

[6]. Hoch AI, Mittal V, Mitra D, Vollmer N, Zikry CA, Leach JK, Biomaterials 2016, 74, 178. [PubMed: 26457835]

[7]. a)Song L, Webb NE, Song YJ, Tuan RS, Stem Cells 2006, 24, 1707; [PubMed: 16574750] b)Law S, Chaudhuri S, Am J Stem Cells 2013, 2, 22. [PubMed: 23671814]

[8]. Poon B, Kha T, Tran S, Dass CR, J Pharm Pharmacol 2016, 68, 139. [PubMed: 26727402]

[9]. James AW, LaChaud G, Shen J, Asatrian G, Nguyen V, Zhang X, Ting K, Soo C, Tissue Eng Part B Rev 2016, 22, 284. [PubMed: 26857241]

[10]. Zakaria SM, Sharif SH, Othman MR, Yang F, Jansen JA, Tissue Eng Part B-Re 2013, 19, 431.

[11]. Lee WH, Loo CY, Van KL, Zavgorodniy AV, Rohanizadeh R, J R Soc Interface 2012, 9, 918. [PubMed: 21957116]

[12]. Marupanthorn K, Tantrawatpan C, Kheolamai P, Tantikanlayaporn D, Manochantr S, Int J Mol Med 2017, 39, 654. [PubMed: 28204808]

[13]. a)Li JY, Mooney DJ, Nat Rev Mater 2016, 1, 16071; [PubMed: 29657852] b)Zhu JM, Marchant RE, Expert Rev Med Devic 2011, 8, 607;c)Kim S, Cui ZK, Kim PJ, Jung LY, Lee M, Acta Biomater 2018, 72, 45; [PubMed: 29597024] d)Fritsch C, Sawala A, Harris R, Maartens A, Sutcliffe C, Ashe HL, Ray RP, J Biol Chem 2012, 287, 5942. [PubMed: 22199351]

[14]. a)Mondal S, Dorozhkin SV, Pal U, Wires Nanomed Nanobi 2018, 10, e1504;b)Uskokovic V, Crit Rev Ther Drug 2015, 32, 1.

[15]. McMillan A, Nguyen MK, Gonzalez-Fernandez T, Ge PL, Yu XH, Murphy WL, Kelly DJ, Alsberg E, Biomaterials 2018, 161, 240. [PubMed: 29421560]

[16]. Dang PN, Herberg S, Varghai D, Riazi H, Varghai D, McMillan A, Awadallah A, Phillips LM, Jeon O, Nguyen MK, Dwivedi N, Yu XH, Murphy WL, Alsberg E, Stem Cell Transl Med 2017, 6, 1644.

[17]. a)Lee EJ, Park SJ, Kang SK, Kim GH, Kang HJ, Lee SW, Jeon HB, Kim HS, Mol Ther 2012, 20, 1424; [PubMed: 22453767] b)Yeh HY, Liu BH, Hsu SH, Biomaterials 2012, 33, 8943. [PubMed: 22985995]

[18]. Dang PN, Dwivedi N, Yu XH, Phillips L, Bowerman C, Murphy WL, Alsberg E, ACS Biomater Sci Eng 2016, 2, 30.

[19]. Ma J, Both SK, Yang F, Cui FZ, Pan J, Meijer GJ, Jansen JA, van den Beucken JJ, Stem Cells Transl Med 2014, 3, 98. [PubMed: 24300556]

[20]. a)Ho SS, Hung BP, Heyrani N, Lee MA, Leach JK, Stem Cells 2018, 36, 1393; [PubMed: 29968952] b)Hung BP, Harvestine JN, Saiz AM, Gonzalez-Fernandez T, Sahar DE, Weiss ML, Leach JK, Biomaterials 2019, 189, 1; [PubMed: 30384124] c)Saiz AM, Gionet-Gonzales MA, Lee MA, Leach JK, Bone 2019, 125, 151; [PubMed: 31102712] d)Gurumurthy B, Bierdeman PC, Janorkar AV, J Biomed Mater Res A 2017, 105, 1230. [PubMed: 27943608]

[21]. Decambron A, Devriendt N, Larochette N, Manassero M, Bourguignon M, El-Hafci H, Petite H, Viateau V, Logeart-Avramoglou D, Tissue Eng Pt A 2019, 25, 642.

[22]. El Bialy I, Jiskoot W, Reza Nejadnik M, Pharm Res 2017, 34, 1152. [PubMed: 28342056]

[23]. Huang BL, Yuan Y, Li T, Ding S, Zhang WJ, Gu YT, Liu CS, Sci Rep 2016, 6, 24323 [PubMed: 27075233]

[24]. a)Vorwald CE, Ho SS, Whitehead J, Leach JK, Methods Mol Biol 2018, 1758, 139; [PubMed: 29679328] b)Whitehead J, Zhang J, Harvestine JN, Kothambawala A, Liu G.-y., Leach JK, Stem Cells 2019, In Press.

[25]. Cummings L, United States of America Patent US 8895707 B2, 2012.

[26]. a)Hoch AI, Binder BY, Genetos DC, Leach JK, Plos One 2012, 7, e35579; [PubMed: 22536411] b)Decaris ML, Leach JK, Ann Biomed Eng 2011, 39, 1174. [PubMed: 21120695]

[27]. Schmittgen TD, Livak KJ, Nat Protoc 2008, 3, 1101. [PubMed: 18546601]

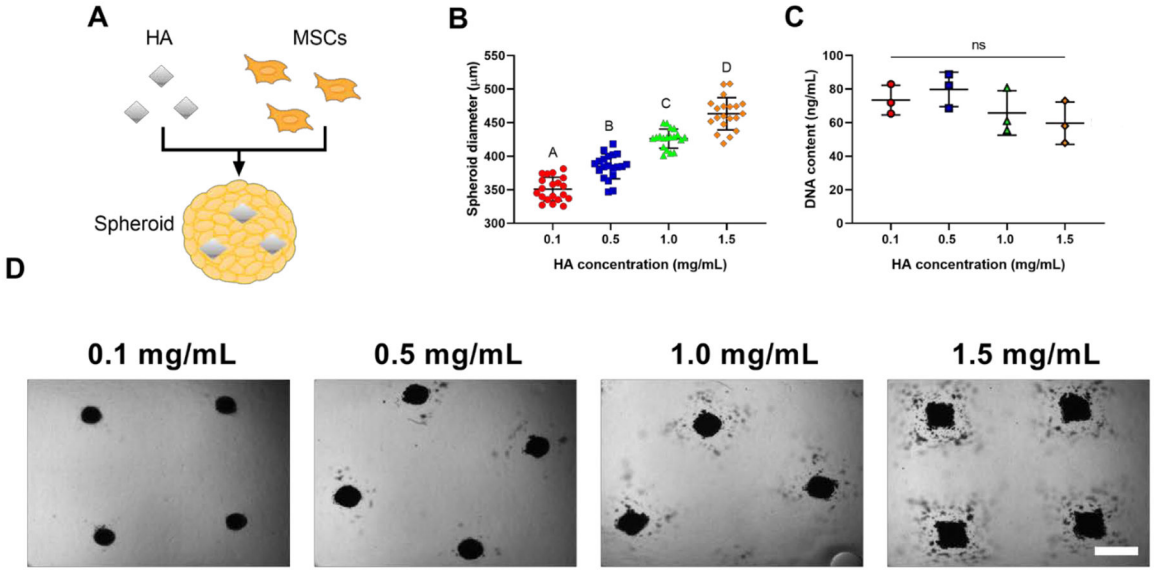

Figure 1.

MSC spheroid morphology and diameter are influenced by HA concentration. **(A)** Schematic of HA incorporation into spheroids. **(B)** Spheroid diameter as a function of HA incorporation (n=20). **(C)** DNA content as a function of HA incorporation (n=3). **(D)** Representative brightfield images of live spheroids containing 0.1–1.5 mg/mL of HA after 48 hours in the microwells. Scale bar represents 500 μm. Groups with different letters are statistically different based on a one-way ANOVA with $p<0.05$. Data are mean ± standard deviation.

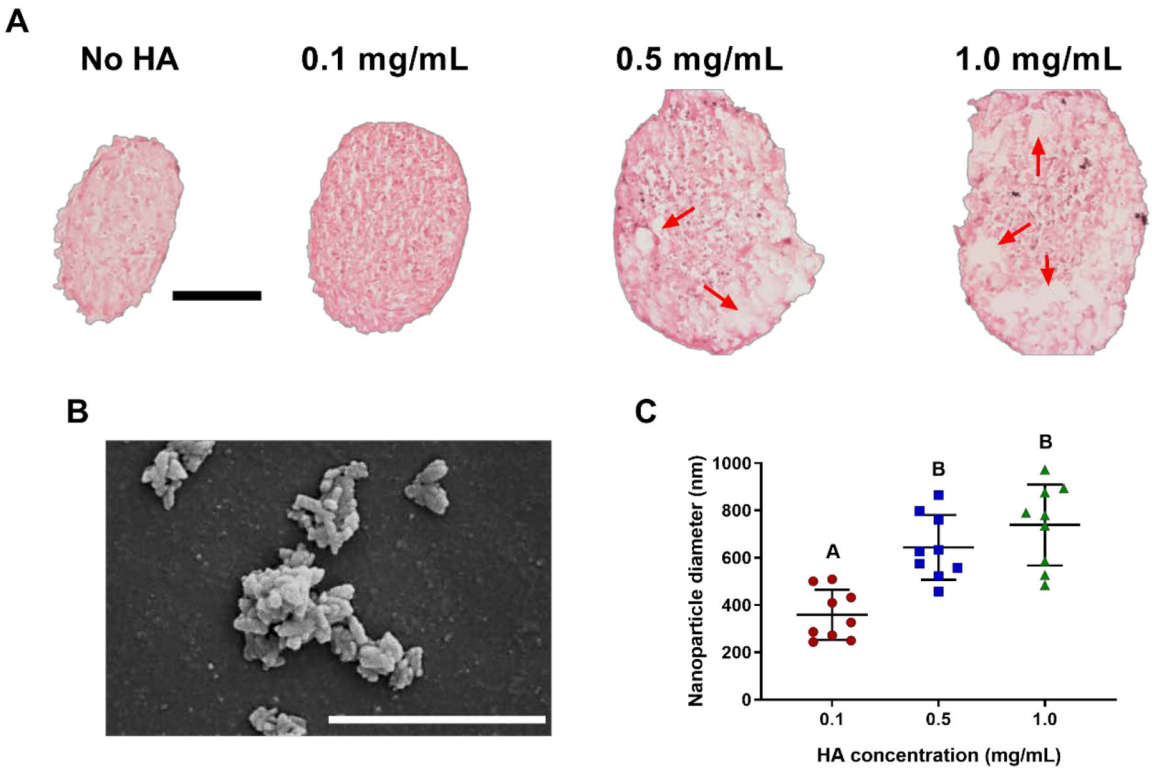

Figure 2.

HA distribution within MSC spheroids is dependent on loading concentration. **(A)** H&E staining of spheroids with varying HA concentrations after 48 hours of spheroid formation. Red arrows indicate voids where HA was present in spheroids. Scale bar represents 100 μm. **(B)** SEM image of HA immediately before incorporation into spheroids. Magnification is 100,000x; scale bar is 1 μm. **(C)** Diameter of HA as a function of concentration immediately before incorporation into spheroids (n=9). Groups with different letters are statistically different based on a one-way ANOVA with $p<0.05$. Data are mean ± standard deviation.

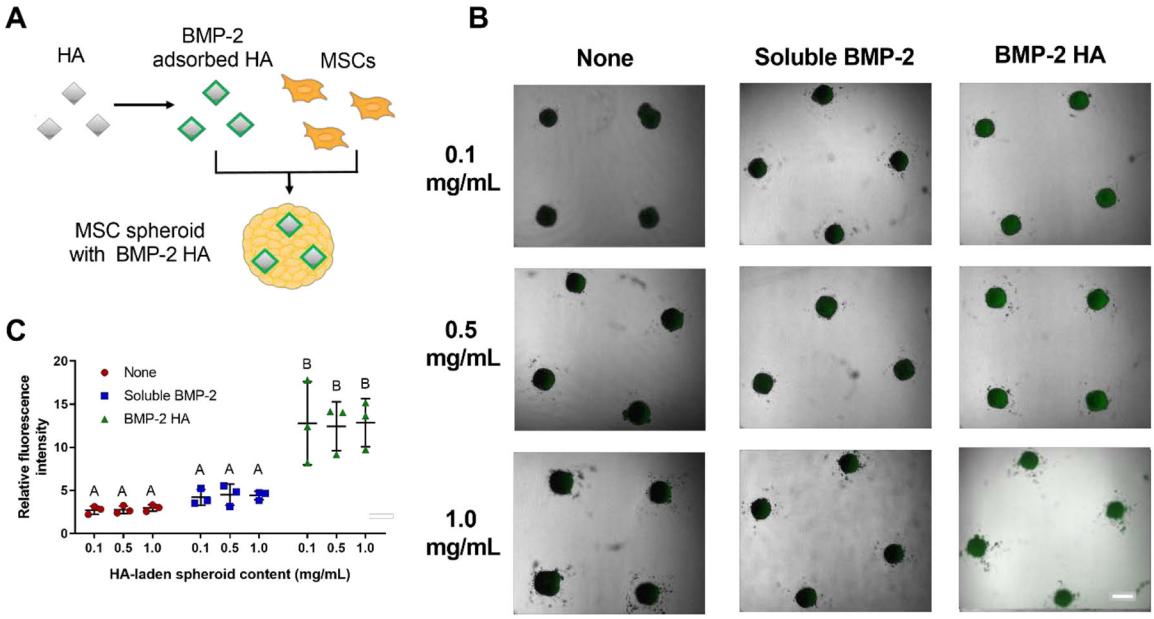

Figure 3.

BMP-2 is observable within MSC spheroids when adsorbed onto HA. **(A)** Schematic of BMP-2 adsorption onto HA and incorporation into spheroids. **(B)** Representative brightfield images with a fluorescence overlay of spheroids with BMP-2 (green) adsorbed onto HA, in culture media, or not present. Scale bar is 500 μm. **(C)** Quantification of the relative fluorescence intensity of spheroids treated with HA alone, HA with soluble BMP-2, or BMP-2 adsorbed onto HA (n=3). Groups with different letters are statistically different based on a one-way ANOVA with $p<0.05$. Data are mean ± standard deviation.

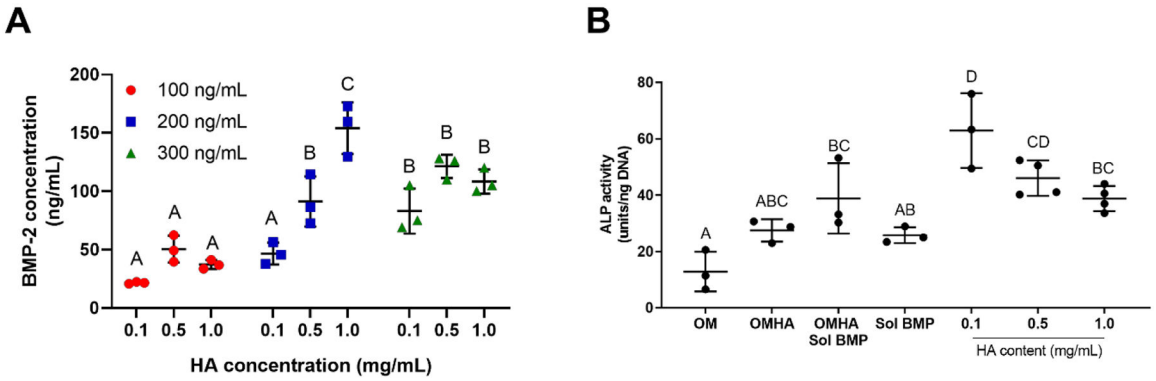

Figure 4.

Measurement of BMP-2 loading and bioactivity. **(A)** Quantification of BMP-2 adsorbed to HA nanoparticles is primarily dependent upon initial BMP-2 concentration (n=3). **(B)** Bioactivity of adsorbed BMP-2 confirmed by measuring ALP activity of W-20–17 cells as a function of HA and BMP-2 treatment (n=3–4). Groups with different letters are statistically different based on a one-way ANOVA with $p<0.05$. Data are mean ± standard deviation.

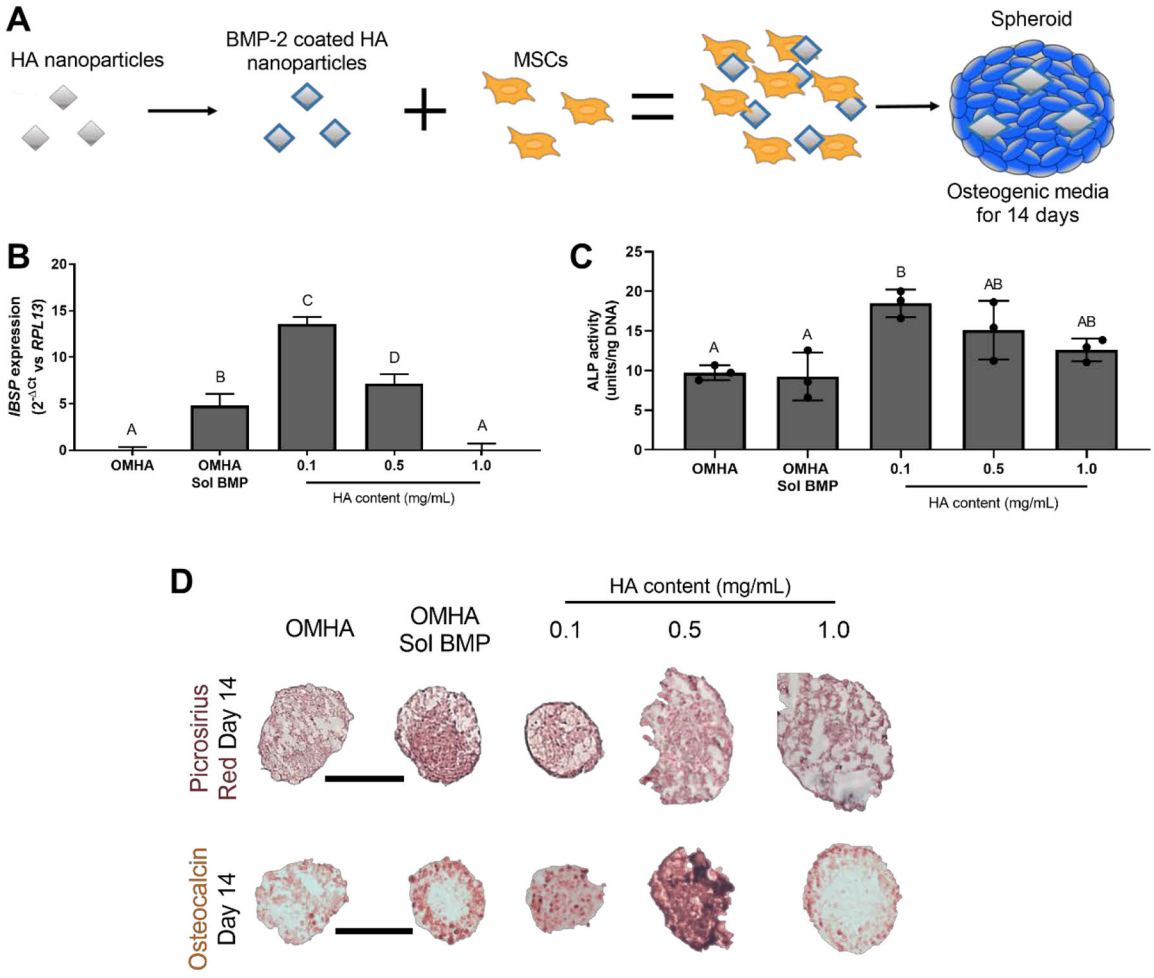

Figure 5.

Localized BMP-2 delivery from HA nanoparticles promotes osteogenic differentiation throughout the spheroid. **(A)** Schematic of MSC spheroid induction with BMP-2 adsorbed onto HA. **(B)** *IBSP* expression in MSC spheroids as a function of BMP-2 and HA treatment after 7 days in osteogenic culture (n=4). **(C)** ALP activity in MSC spheroids at day 7 (n=3). **(D)** Representative histology demonstrating picrosirius red (top) and osteocalcin staining (bottom) of spheroids at day 14. Scale bars are 200 μm. Groups with different letters are statistically different based on a one-way ANOVA with $p<0.05$. Data are mean ± standard deviation.

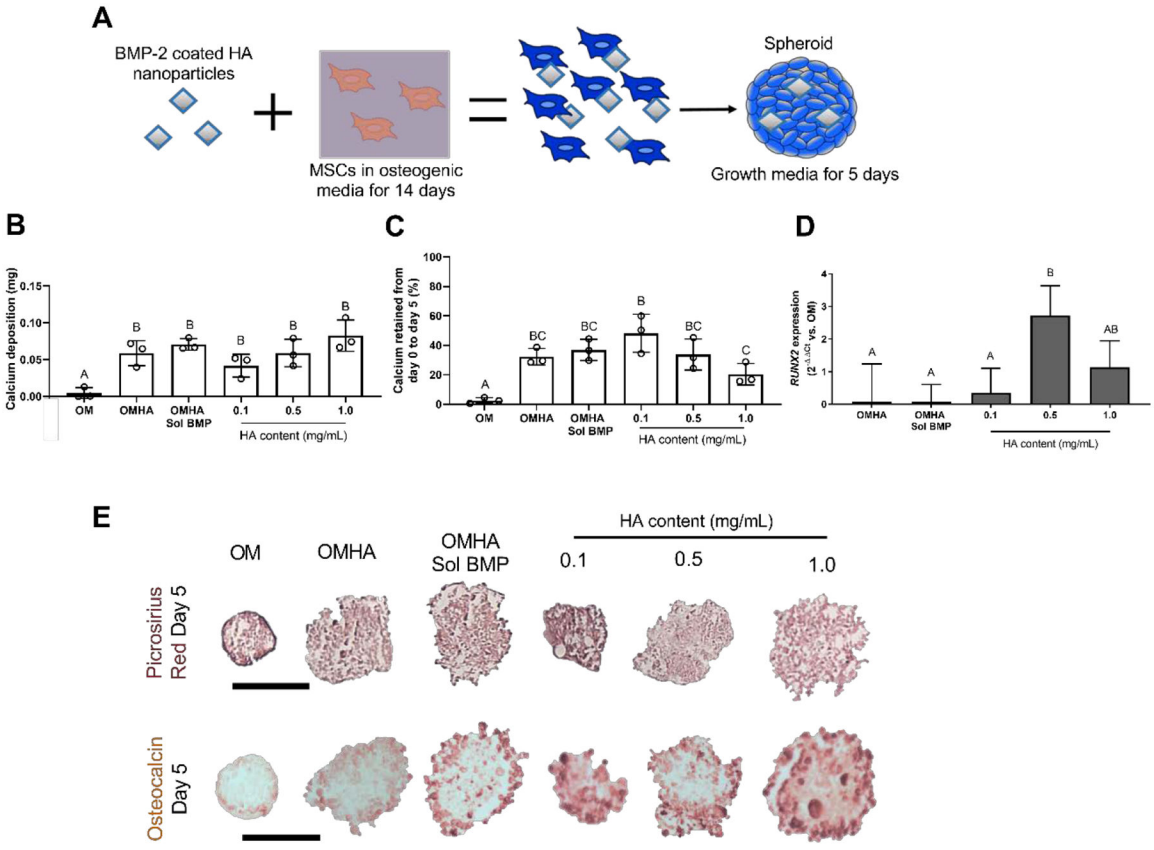

Figure 6.

Localized BMP-2 delivery by HA enhances the retention of the osteogenic phenotype after removal of soluble osteogenic cues. **(A)** Schematic of studies to evaluate osteogenic retention in spheroids. **(B)** Total calcium after 5 days in growth media (n=3). **(C)** The percent change in calcium from osteogenic induction to 5 days in media lacking additional osteogenic supplements (n=3). **(D)** *RUNX2* expression in MSC spheroids as a function of BMP-2 and HA treatment compared to expression in OM after 5 days in media lacking additional osteogenic supplements (n=4). **(E)** Representative histology of picrosirius red (top) and osteocalcin staining (bottom) in spheroids after 5 days in growth media. Scale bars are 200 μm. Groups with different letters are statistically different based on a one-way ANOVA with $p<0.05$. Data are mean ± standard deviation.

Table 1:

Description of spheroid contents and abbreviations used in this study

Abbreviation	Spheroid Contents
OM	formed and maintained in osteogenic media
OMHA	osteogenic media with 0.5 mg/mL HA incorporated
OHMA Sol BMP	osteogenic media with 0.5 mg/mL HA incorporated and soluble BMP-2 (200 ng/mL) added to the culture medium
Sol BMP	soluble BMP-2 (200 ng/mL) added to osteogenic media
0.1	BMP-2 adsorbed onto 0.1 mg/mL of HA incorporated into spheroids
0.5	BMP-2 adsorbed onto 0.5 mg/mL of HA incorporated into spheroids
1.0	BMP-2 adsorbed onto 1.0 mg/mL of HA incorporated into spheroids